Journal of Structural Engineering. Submitted December 15, 2011; accepted August 2, 2012;
posted ahead of print August 13, 2012. doi:10.1061/(ASCE)ST.1943-541X.0000697

Retracted: Appropriate modulating function for the simulation of non-stationary wind velocity

Jinhua Li*

Department of Civil Engineering, East China Jiaotong University, No.808 Shuanggang St., Nanchang 330013, P. R. China ; formerly, Department of Civil Engineering, Shanghai University, No.149 Yanchang Rd., Shanghai 200072, P. R. China

Abstract: Following the theory of evolutionary power spectral density (EPSD) for non-stationary stochastic processes, it is anticipated that the non-stationary fluctuating wind velocity can be generated by resorting to a deterministic modulating function used to modulate the stationary fluctuating wind velocity. Naturally, the key to the reproduction of non-stationary fluctuating wind velocity lies in seeking out an effective deterministic modulating function. Attention has been focused in the present study on how to obtain appropriate deterministic modulating function enabled to modulate stationary fluctuating wind velocity. According to the Kaimal power spectrum, a deterministic modulating function is deduced in detail in the fourth section of this paper. In the same way, other modulating functions can be also obtained based on different power spectra, such as Davenport power spectrum, Simiu power spectrum and so on. In the process of simulating non-stationary wind velocities through the derived deterministic modulating function, spline interpolation is introduced herein to reduce the increasing number of Cholesky decomposition of the time-varying spectral density matrix. Results obtained from the fifth section of this paper corroborate the effectiveness and faithfulness of the simulated non-stationary stochastic processes, and show that the derived modulating function can capture

Journal of Structural Engineering. Submitted December 15, 2011; accepted August 2, 2012;
posted ahead of print August 13, 2012. doi:10.1061/(ASCE)ST.1943-541X.0000697

fully the non-stationarity of wind velocities.

***Keywords*:** Non-stationary wind velocity; Deterministic modulating function; power spectrum; Spectral representation; Spline interpolation.

---

*Corresponding author**:** Dr. Jinhua Li

Tel.: +86-135-7628-3532;

E-mail: Jinhua@ecjtu.edu.cn

Introduction

Extreme wind events in many districts around the world are caused by severe convective thunderstorm winds and typhoon-induced winds, which are responsible for significant structural damage and failures. This sort of wind flow varies significantly from the traditional atmospheric boundary layer wind flows in light of its unique mean wind speed vertical profile, rapid time-varying mean wind speed, and spatially strongly correlated wind fluctuations. Extreme winds exhibit the transient non-stationary features which may remarkably influence wind-structure interaction and wind load effects on buildings (Chen 2008). More specifically, not only does the load quantity change with time and frequency, but the direction in which these loads impinge on structures also changes, thus further complicating the load and performance assessment process. Apparently, in order to obtain more reliable wind-resistant designs, it is imperative and of practical interest to capture the transient non-stationary phenomena in thunderstorm downbursts and typhoon-induced winds with resorting to the numerical simulation techniques. Naturally, it is envisaged to develop an efficient yet accurate simulation method of transient non-stationary

Journal of Structural Engineering. Submitted December 15, 2011; accepted August 2, 2012;
posted ahead of print August 13, 2012. doi:10.1061/(ASCE)ST.1943-541X.0000697

winds.

Monte Carlo-based simulation approaches, which may generate the sample functions with the probabilistic characteristics of target stochastic process, have been widely employed in simulating the stochastic processes (Li and Li 2012). The scope of simulations spans uni-dimensional to multi-dimensional fields; univariate to multivariate processes; homogeneous to non-homogeneous fields; stationary to non-stationary; Gaussian to non-Gaussian; and conditional to unconditional cases. To date, the following approaches are available for the simulation of stochastic processes**:** (1) auto-regressive (AR) model in the white noise filtration method (WNFM), such as Spanos and Mignolet (1987), Grigoriu *et al.* (1988), Yeh and Wen (1990), Novak *et al*. (1995), and Li and Li (2011); (2) move-regressive (MA) model in the WNFM, e**.**g**.** Mignolet and Spanos (1990), Spanos and Mignolet (1990); (3) auto-regressive moving average (ARMA) model in the WNFM, for example, Kozin (1988), Kareem and Li (1992), Rossi *et al*. (2004), and Li and Li (2012); and (4) spectral representation, referred thereinafter to as the SR, method, for instance, Grigoriu (1993), Li and Kareem (1991), Deodatis (1996), Chen and Letchford (2005a), and Li *et al*. (2011) . AR and MA can be included in ARMA model (Mignolet and Spanos 1992; Spanos and Mignolet 1992), which is a counterpart to the SR method. It is noted that the computational efficiency of the SR method is rather low. A possible remedy to this issue is to introduce the fast Fourier transform (FFT) algorithm into the SR method. Yang (1972) showed that the FFT algorithm can remarkably enhance the computational efficiency of the SR method, and furthermore developed a formula to simulate the random envelop processes. Wittig and Sinhat (1975) demonstrated that the SR

Journal of Structural Engineering. Submitted December 15, 2011; accepted August 2, 2012;
posted ahead of print August 13, 2012. doi:10.1061/(ASCE)ST.1943-541X.0000697

method combined with the FFT algorithm appears to be more than an order of magnitude faster than other simulation methods. Further, Li and Kareem (1997) used a computationally efficient FFT-based approach to simulate the multivariate Gaussian non-stationary random processes (Regarding the reproduction of seismic ground motions) with the prescribed evolutionary spectral description. Unfortunately, the FFT algorithm is not directly applicable to the non-stationary case. However, when the modulating function is a deterministic time function, the FFT algorithm may then be employed for the simulation of the non-stationary stochastic process. The SR method has very high demands on both the computer memory and computational speed but does not have the problem of model selection. Likewise, it is easy to implement and moreover, render high accuracy. Therefore, the SR method has yet been receiving increasing attention in simulating the multivariate stochastic processes. In view of these, the SR method will be taken into consideration in this paper.

It is known that the simulation of non-stationary stochastic processes may be simplified via representing non-stationary stochastic processes in terms of stationary processes modulated by slowly varying deterministic functions, referred to as uniformly modulated stationary processes. Saragoni and Hart (1973) partitioned the non-stationary stochastic process into several segments and then proposed a piecewise stationary model. Later, an extension of the Saragoni-Hart model was made by Der Kiureghian and Crempien (1989). They represented the model as a summation of modulated banded white noise. Li and Kareem (1991) also used the modulated stationary stochastic process concept. A non-stationary process was expressed as a sum of mutually correlated stationary processes modulated by a deterministic time function. The spectrum of the

Journal of Structural Engineering. Submitted December 15, 2011; accepted August 2, 2012;
posted ahead of print August 13, 2012. doi:10.1061/(ASCE)ST.1943-541X.0000697

stationary processes and the deterministic modulating time function can be derived through matching a prescribed evolutionary spectrum. Liang *et al*. (2007) presents a rigorous derivation of a previously known formula for simulation of one-dimensional, univariate, non-stationary stochastic processes integrating Priestley's evolutionary SR theory. The utilization of the SR method thus is believed to be possible in simulating the non-stationary stochastic process.

It is worth pointing herein out that most simulations of the non-stationary stochastic processes have involved around the reproduction of seismic ground motions known to be highly non-stationary (Kareem 2008). The literature (Kareem 2008) presents an overview of the simulation of seismic ground motions. Recent research works on non-stationary winds mainly consist of the contributions by Wang and Kareem (2004; 2005), Xu and Chen (2004), Chen and Letchford (2004; 2005b; 2007), Chay *et al*. (2006) and Chen (2008). In some literatures (Chen and Letchford 2004; Chen 2008), the function of time-varying mean wind speed multiplying a constant is given directly as the modulating function without detailed derivation and prove. Furthermore, the given modulating function is only a function of time. According to the theory of evolutionary power spectra, a modulating function should be the function of time and frequency, namely non-uniform modulating function. Due to the lack of the valid modulating function, the numerical simulation of transient non-stationary winds has been rather limited. Therefore, it is significant to find the appropriate modulating function for the simulation of non-stationary fluctuating winds.

This study deals with the numerical simulation of non-stationary wind velocity fields through the SR method coupled with the spline interpolation algorithm (SIA), which is aimed at

Journal of Structural Engineering. Submitted December 15, 2011; accepted August 2, 2012;
posted ahead of print August 13, 2012. doi:10.1061/(ASCE)ST.1943-541X.0000697

reducing the increasing number of the Cholesky decomposition of power spectral matrix with the duration of simulation. Apparently, an important work of the present paper is to present an efficacious approach to obtain a proper deterministic modulating function utilized to modulate non-uniformly the stationary fluctuating wind velocity. Eventually, the present methodology is applied to the reproduction of fluctuating wind speed time series at three dissimilar points envisaged of non-stationary wind velocities.

SR method of non-stationary stochastic processes

Take into account a multivariate non-stationary stochastic process with the components, respectively, being $u_1(t)$, $u_2(t)$, $\cdots$,$u_n(t)$, and furthermore with the mean value equal to zero, more specifically,

$$E[u_j(t)] = 0 \quad (j = 1, 2, \cdots, \boldsymbol{n}) \tag{1}$$

The correlation matrix is given by

$$\mathbf{R}^0(t, t+\tau) = \begin{bmatrix} R^0_{11}(t, t+\tau) & R^0_{12}(t, t+\tau) & \cdots & \boldsymbol{R}^0_{1n}(t, t+\tau) \\ R^0_{21}(t, t+\tau) & R^0_{22}(t, t+\tau) & \cdots & \boldsymbol{R}^0_{2n}(t, t+\tau) \\ \vdots & \vdots & \ddots & \vdots \\ R^0_{n1}(t, t+\tau) & R^0_{n2}(t, t+\tau) & \cdots & \boldsymbol{R}^0_{nn}(t, t+\tau) \end{bmatrix} \tag{2}$$

Simultaneously, the power spectral density (PSD) matrix is written as follows**:**

$$\mathbf{S}^0(\omega, t) = \begin{bmatrix} S^0_{11}(\omega, t) & S^0_{12}(\omega, t) & \cdots & S^0_{1n}(\omega, t) \\ S^0_{21}(\omega, t) & S^0_{22}(\omega, t) & \cdots & S^0_{2n}(\omega, t) \\ \vdots & \vdots & \ddots & \vdots \\ S^0_{n1}(\omega, t) & S^0_{n2}(\omega, t) & \cdots & S^0_{nn}(\omega, t) \end{bmatrix} \tag{3}$$

Apparently, in relation to the non-stationary stochastic processes, the correlation matrix is a function of two time instants t and $t+\tau$ (More specifically, t represents the time and $t+\tau$

Journal of Structural Engineering. Submitted December 15, 2011; accepted August 2, 2012;
posted ahead of print August 13, 2012. doi:10.1061/(ASCE)ST.1943-541X.0000697

denotes the time lag.), while the PSD matrix is a function of both frequency ω and time t. Among existing definitions of non-stationary spectra, the most widely used is probably Priestley's evolutionary power spectral density (EPSD) (Priestley 1965; Priestley 1988). By resorting to the theory of evolutionary power spectra for non-stationary stochastic processes, the PSD functions of non-stationary stochastic processes $u_1(t),\ u_2(t),\ \cdots\ ,u_n(t)$ are defined as follows:

$$S_j^0(\omega,t) = \left|A_j(\omega,t)\right|^2 S_j(\omega) \quad (j=1,2,3,\cdots,n) \tag{4}$$

$$S_{jk}^0(\omega,t) = A_j^*(\omega,t)\,A_k(\omega,t)\sqrt{S_j(\omega)}\sqrt{S_k(\omega)}\,\Gamma_{jk}(\omega) \quad (j,k=1,2,3,\cdots,n, j\neq k) \tag{5}$$

In the preceding Eq.(5), the star $*$ denotes complex conjugate; $A_j(\omega,t)\ (j=1,2,3,\cdots,n)$ refer to the modulating functions; $S_j(\omega)\ (j=1,2,3,\cdots,n)$ represent the PSD functions of stationary stochastic processes; and $\Gamma_{jk}\ (j,k=1,2,3,\cdots,n, j\neq k)$ is the coherence functions. It is worth pointing out that Eqs.(4) and (5) mean that the modulating function $A_j(\omega,t)$ measures the change in the EPSD with respect to the stationary PSD function $S_j(\omega)$. Likewise, the following two transformations display the relationship between the elements of the correlation matrix $\mathbf{R}^0(t,t+\tau)$ and the corresponding elements of the PSD matrix $\mathbf{S}^0(\omega,t)$.

$$R_{jj}(t,t+\tau) = \int_{-\infty}^{+\infty} S_j^0(\omega,t)\cdot e^{i\omega\tau}\,d\omega \quad (j=1,2,3,\cdots,n) \tag{6}$$

$$R_{jk}(t,t+\tau) = \int_{-\infty}^{+\infty} S_{jk}^0(\omega,t)\cdot e^{i\omega\tau}\,d\omega \quad (j,k=1,2,3,\cdots,n, j\neq k) \tag{7}$$

In order to simulate the one-dimensional multivariate non-stationary stochastic process $u_j(t)\ (j=1,2,\cdots,n)$, the PSD matrix $\mathbf{S}^0(\omega,t)$ must be first decomposed under consideration into a product of two matrices, which is given by

$$\mathbf{S}^0(\omega,t) = \mathbf{H}(\omega,t)\,\mathbf{H}^{T*}(\omega,t) \tag{8}$$

Journal of Structural Engineering. Submitted December 15, 2011; accepted August 2, 2012;
posted ahead of print August 13, 2012. doi:10.1061/(ASCE)ST.1943-541X.0000697

In the preceding equation, the superscript $T*$ represents the complex conjugate transpose of a matrix; and $\mathbf{H}(\omega,t)$ is a lower triangular matrix below.

$$\mathbf{H}(\omega,t)=\begin{bmatrix} H_{11}(\omega,t) & 0 & \cdots & 0 \\ H_{21}(\omega,t) & H_{22}(\omega,t) & \cdots & 0 \\ \vdots & \vdots & \ddots & \vdots \\ H_{n1}(\omega,t) & H_{n2}(\omega,t) & \cdots & H_{nn}(\omega,t) \end{bmatrix} \tag{9}$$

in which, all the diagonal elements are the real and non-negative functions of frequency ω; and it is generally admitted that the off-diagonal elements are the complex functions of frequency ω. $\mathbf{H}(\omega,t)$can be solved through the Cholesky decomposition of $\mathbf{S}^0(\omega,t)$.

Again, it is assumed that the off-diagonal element $H_{jm}(\omega,t)$ may be written in the polar form as follows**:**

$$H_{jm}(\omega,t)=\left|H_{jm}(\omega,t)\right|e^{i\vartheta_{jm}(\omega,t)} \quad (j=1,2,\cdots,n,\ k=1,2,\cdots,n,\ j>k) \tag{10}$$

where

$$\vartheta_{jm}(\omega,t)=\tan^{-1}\frac{\mathrm{Im}\left[H_{jm}(\omega,t)\right]}{\mathrm{Re}\left[H_{jm}(\omega,t)\right]} \tag{11}$$

In the preceding equation, Im and Re refer to the imaginary and real parts of a complex number, respectively.

According to Deodatis (1996), the non-stationary stochastic process $u_j(t)\,(j=1,2,\cdots,n)$ can be reproduced by the following series as $N\to\infty$.

$$u_j(t)=2\sqrt{\Delta\omega}\sum_{m=1}^{n}\sum_{l=1}^{N}\left|H_{jm}(\omega_l,t)\right|\cos\left[\omega_l t-\vartheta_{jm}(\omega_l,t)+\Phi_{ml}\right] \quad (j=1,2,\cdots,n) \tag{12}$$

where the circular frequency $\omega_l=l\Delta\omega\,(l=1,2,3,\cdots,N)$; N refers to the sufficiently large dividing number of circular frequency; $\Delta\omega=\omega_{up}/N$ denotes the circular frequency increment; ω_{up} refers to the upper cutoff circular frequency, with the condition that, when $\omega_l>\omega_{up}$, the

Journal of Structural Engineering. Submitted December 15, 2011; accepted August 2, 2012;
posted ahead of print August 13, 2012. doi:10.1061/(ASCE)ST.1943-541X.0000697

value of $H_{jm}(\omega)$ becomes trivial; Φ_{ml} represents the sequences of independent random phase angles, distributed uniformly over the interval $[0, 2\pi]$.

It is worth mentioning herein that in accordance with the central limit theorem (Shinozuka and Deodatis 1991), the simulated non-stationary stochastic process $u_j(t)$ $(j=1,2,\cdots,n)$ is an asymptotically Gaussian as $N \to \infty$.

Introducing SIA into SR method

Since the Cholesky decomposition has to be conducted separately for each frequency ω_l at each time instant t, the total number of implementing the Cholesky decomposition with respect to Eq.(12) is equivalent to $n \times N$. Therefore, the computational effort of the SR method is rather tremendous for the simulation of non-stationary stochastic processes. Likewise, for the multivariate non-stationary stochastic processes with the phase angles, the cross PSD matrix $S^0_{jk}(\omega,t)$ is a complex matrix. Accordingly, the element $H_{jm}(\omega,t)=\left|H_{jm}(\omega,t)\right| e^{i\vartheta_{jm}}$ of the obtained lower triangular matrix $H(\omega,t)$ based on the Cholesky decomposition is also complex. Notice that $\left|H_{jm}(\omega,t)\right|$ varies continuously with the circle frequency at each time instant t. It is therefore inferred that as long as $\left|H_{jm}(\omega,t)\right|$ at some appropriate circle frequency points are calculated, $\left|H_{jm}(\omega,t)\right|$ at other circle frequency points can then be obtained by using the cubic SIA. Since the spline function possesses the advantages of both the smoothness and continuance, it has been widely utilized to interpolate and fit data in engineering.

The following is the framework that the SIA is introduced into the SR method for the

Journal of Structural Engineering. Submitted December 15, 2011; accepted August 2, 2012; posted ahead of print August 13, 2012. doi:10.1061/(ASCE)ST.1943-541X.0000697

improvement of computational efficiency.

First, it is assumed that the circle frequency interval $[0, \omega_u]$ is evenly divided into r sub-intervals by using $r-1$ circle frequencies $\omega_1, \omega_2, \cdots, \omega_{r-1}$ but content with $0=\omega_0<\omega_1<\cdots<\omega_r=\omega_u$. With that, the corresponding $\left|H_{jm}(\omega_i,t)\right|$ ($i=0,\ 1,\ 2,\ \cdots,\ r$) can be calculated.

Then, it is assumed that both $\tilde{H}_{jm}(\omega_i,t)=\left|H_{jm}(\omega_i,t)\right|$ ($i=0,\ 1,\ 2,\ \cdots,\ r$) and second continuous derivative $\tilde{H}''_{jm}(\omega_i,t)=P_{it}$ ($i=0,\ 1,\ 2,\ \cdots,\ r$), consequently, $\tilde{H}_{jm}(\omega,t)$ at other circle frequency points can be calculated by resorting to the cubic spline interpolation, more specifically,

$$\tilde{H}_{jm}(\omega,t)=\begin{cases}
\dfrac{r}{6\omega_u}\left[(\omega_1-\omega)^3P_{0t}+(\omega-\omega_0)^3P_{1t}\right]+\left[\tilde{H}_{jm}(\omega_0,t)-\dfrac{\omega_u^2}{6r^2}P_{0t}\right]\dfrac{\omega_1-\omega}{\omega_u}r \\
+\left[\tilde{H}_{jm}(\omega_1,t)-\dfrac{\omega_u^2}{6r^2}P_{1t}\right]\dfrac{\omega-\omega_0}{\omega_u}r & (\omega_0\le\omega\le\omega_1) \\
\dfrac{r}{6\omega_u}\left[(\omega_2-\omega)^3P_{1t}+(\omega-\omega_1)^3P_{2t}\right]+\left[\tilde{H}_{jm}(\omega_1,t)-\dfrac{\omega_u^2}{6r^2}P_{1t}\right]\dfrac{\omega_2-\omega}{\omega_u}r \\
+\left[\tilde{H}_{jm}(\omega_2,t)-\dfrac{\omega_u^2}{6r^2}P_{2t}\right]\dfrac{\omega-\omega_1}{\omega_u}r & (\omega_1\le\omega\le\omega_2) \\
\cdots\cdots & \\
\dfrac{r}{6\omega_u}\left[(\omega_r-\omega)^3P_{(r-1)t}+(\omega-\omega_{r-1})^3P_{rt}\right]+\left[\tilde{H}_{jm}(\omega_{r-1},t)-\dfrac{\omega_u^2}{6r^2}P_{(r-1)t}\right]\dfrac{\omega_r-\omega}{\omega_u}r \\
+\left[\tilde{H}_{jm}(\omega_r,t)-\dfrac{\omega_u^2}{6r^2}P_{rt}\right]\dfrac{\omega-\omega_{r-1}}{\omega_u}r & (\omega_{r-1}\le\omega\le\omega_r)
\end{cases} \tag{13}$$

In the preceding equation, the second continuous derivative P_{it} ($i=0,\ 1,\ 2,\ \cdots,\ r$) may be determined by using the three-moment equation.

On introducing the SIA into $\left|H_{jm}(\omega)\right|$, Eq.(12) for the simulation of the multivariate non-stationary stochastic processes can be rewritten as follows:

Journal of Structural Engineering. Submitted December 15, 2011; accepted August 2, 2012;
posted ahead of print August 13, 2012. doi:10.1061/(ASCE)ST.1943-541X.0000697

$$u_j(t) = 2\sqrt{\Delta\omega}\sum_{m=1}^{n}\sum_{l=1}^{N}\tilde{H}_{jm}(\omega_l)\cos\left[\omega_l t - \vartheta_{jm}(\omega_l,t) + \Phi_{ml}\right] \quad (j = 1,2,\cdots,n) \tag{14}$$

Derivation of deterministic modulating function

In the conventional approaches for the prediction of wind-induced response of slender structures, the boundary layer longitudinal wind velocity $f(t)$ at a given height is generally assumed to be an ergodic random process, which consists of a constant mean wind velocity component $\bar{U}$ and a longitudinal fluctuating wind velocity component $u(t)$ in the form:

$$f(t) = \bar{U} + u(t) \tag{15}$$

It is worth pointing herein out that the term "mean" refers to an average over a time interval T, thus effectively meaning that the mean wind velocity component is given by the following equation:

$$\bar{U} = \frac{1}{T}\int_0^T f(t)\,dt \tag{16}$$

In the preceding equation, generally, T is taken as 1 h or 10 min with respect to wind effects on structures, correspondingly leading to the so-called hourly or 10 min mean wind velocity (Lawsoon 1980).

However, the boundary layer wind measured during both thunderstorm and typhoon may not comply with the assumption of the ergodic or stationary random process (Kareem 2008). A recent preliminary study (Xu and Chen 2004) of non-stationary wind data recorded in the field during a nearby typhoon reveals that the mean wind velocity over 1 h often takes on a significant temporal (slowly time-varying) trend. On the basis of this situation, a non-stationary wind model has been put forward by Xu and Chen (2004). This model (which is taken into

Journal of Structural Engineering. Submitted December 15, 2011; accepted August 2, 2012;
posted ahead of print August 13, 2012. doi:10.1061/(ASCE)ST.1943-541X.0000697

consideration in the present paper) means that the non-stationary wind velocity is viewed as a deterministic time-varying mean wind velocity $\tilde{U}(t)$ plus a fluctuating wind velocity $u(t)$ that can be modeled as a zero-mean stationary or non-stationary random process, which has the form:

$$f(t) = \tilde{U}(t) + u(t) \tag{17}$$

It is known that the stationary fluctuating random process admits the well-known spectral representation (e.g., Cramer and Leadbetter 1967) below.

$$u(t) = \int_{-\infty}^{+\infty} e^{i\omega t} d\,Z(\omega) \tag{18}$$

whereas the non-stationary fluctuating random process can be formulated as follows:

$$u(t) = \int_{-\infty}^{+\infty} A(\omega,t)\, e^{i\omega t}\, d\,Z(\omega) \tag{19}$$

where $A(\omega,t)$ is a deterministic modulating function with two variables ω and t; and $Z(\omega)$ represents a spectral process with orthogonal increments which has a distribution function in the interval $(-\infty,+\infty)$.

Obviously, unlike the simulation of stationary stochastic processes, an appropriate deterministic modulating function needs to be predetermined in simulating the non-stationary fluctuating wind velocity.

Time-varying PSD function

Arbitrary non-stationary wind velocity during the time $[0,T]$ can be divided into $n=T/\Delta t$ segments. For one segment with $[\,t_1, t_1+\Delta t\,]$, the time-varying mean wind velocity $\tilde{U}_{z_j}(t) \approx \tilde{U}_{z_j}(t_1)$, and the time-varying PSD function $G_{z_j z_j}(\omega,t) \approx G_{z_j z_j}(\omega,t_1)$ when the interval

Journal of Structural Engineering. Submitted December 15, 2011; accepted August 2, 2012;
posted ahead of print August 13, 2012. doi:10.1061/(ASCE)ST.1943-541X.0000697

Δt is very transitory. Therefore, the segment is considered as stationary wind velocity with mean wind velocity $U_{z_j} = \tilde{U}_{z_j}(t_1)$ and PSD function $S_{z_j z_j}(\omega) = G_{z_j z_j}(\omega, t_1)$.

In order to model the two-sided PSD function $G_{z_j z_j}(\omega, t_1)$ of the approximately stationary wind velocity fluctuations with transitory interval $[t_1, t_1 + \Delta t]$, the expression proposed by Kaimal *et al.* (1972) is taken into consideration herein, which is given by

$$\begin{cases} G_{z_j z_j}(\omega, t_1) = \dfrac{1}{2}\dfrac{200}{2\pi} u_*^2 \dfrac{z_j}{U_{z_j}} \dfrac{1}{\left[1 + 50\dfrac{\omega\, z_j}{2\pi U_{z_j}}\right]^{5/3}} \\ \qquad\qquad = \dfrac{1}{2}\dfrac{200}{2\pi} u_*^2(t_1) \dfrac{z_j}{\tilde{U}_{z_j}(t_1)} \dfrac{1}{\left[1 + 50\dfrac{\omega\, z_j}{2\pi \tilde{U}_{z_j}(t_1)}\right]^{5/3}} \\ u_*(t_1) = \dfrac{\kappa}{\ln\left(\dfrac{z_j}{z_0}\right)} U_{Z_j} = \dfrac{\kappa}{\ln\left(\dfrac{z_j}{z_0}\right)} \tilde{U}_{Z_j}(t_1) \end{cases} \tag{20}$$

According to the logarithmic law, U_{z_k} at the height z_k can be calculated as

$$U_{z_k} = \left[\frac{\ln(z_k / z_0)}{\ln(z_j / z_0)}\right] U_{z_j} = \left[\frac{\ln(z_k / z_0)}{\ln(z_j / z_0)}\right] \tilde{U}_{z_j}(t_1) = \tilde{U}_{z_k}(t_1) \tag{21}$$

Simultaneously, the coherence function between the velocity fluctuations at two different heights z_j and z_k proposed by Davenport (1968) is taken into consideration in the present paper, which is given by

$$\Gamma(\omega, t_1) = Coh(\omega) = \exp\left[-\frac{\omega}{2\pi}\frac{C_z |z_k - z_j|}{\frac{1}{2}(U_{z_k} + U_{z_j})}\right] = \exp\left[-\frac{\omega}{\pi}\frac{C_z |z_k - z_j|}{\tilde{U}_{z_k}(t_1) + \tilde{U}_{z_j}(t_1)}\right] \tag{22}$$

in which C_z is a constant that may generally be set to be equal to 10 for structural design

Journal of Structural Engineering. Submitted December 15, 2011; accepted August 2, 2012;
posted ahead of print August 13, 2012. doi:10.1061/(ASCE)ST.1943-541X.0000697

purposes (Kristensen and Jensen 1979; Simiu and Scanlan 1986).

In regard of the stationary fluctuating wind velocity, the phase angle $\theta_{jk}(\omega)$ can be represented in the form suggested by Di Paola (1998) as

$$\theta_{jk}(\omega)=\frac{\omega(z_j-z_k)}{\upsilon_{app}^{(j,k)}} \tag{23}$$

Likewise, the apparent velocity of waves can be assumed to be the following form given by Simiu and Scanlan (1986).

$$\upsilon_{app}^{(j,k)}=\frac{\pi(U_{z_k}+U_{z_j})}{C_\theta} \tag{24}$$

In the preceding equation, C_θ refers to an appropriate coefficient that has to be determined from experimental data. In the present paper, $C_\theta=5.5$ in the literature (Peil and Telljohann 1996) is taken into account.

Employing Eqs.(23) and (24), we compute that

$$\theta_{jk}(\omega,t_1)=\theta_{jk}(\omega)=\frac{\omega(z_j-z_k)}{\upsilon_{app}^{(j,k)}}=\frac{\omega}{\pi}\frac{C_\theta(z_j-z_k)}{U_{z_k}+U_{z_j}}=\frac{\omega}{\pi}\frac{C_\theta(z_j-z_k)}{\tilde{U}_{z_k}(t_1)+\tilde{U}_{z_j}(t_1)} \tag{25}$$

Hence, the cross PSD function $G_{z_jz_k}(\omega,t_1)$ of the stationary wind velocity fluctuations in $[t_1,t_1+\Delta t]$ can then be determined as follows:

$$\begin{aligned}G_{z_jz_k}(\omega,t_1)&=\Gamma(\omega,t_1)\sqrt{\left[G_{z_jz_j}(\omega,t_1)\right]\left[G_{z_kz_k}(\omega,t_1)\right]}\;e^{-i\theta_{jk}(\omega,\,t_1)}\\&=\exp\left[-\frac{\omega}{\pi}\frac{C_z\left|z_k-z_j\right|}{\tilde{U}_{z_j}(t_1)+\tilde{U}_{z_k}(t_1)}\right]\sqrt{\frac{1}{2}\frac{200}{2\pi}u_*^2(t_1)\frac{z_j}{\tilde{U}_{z_j}(t_1)}\frac{1}{\left[1+50\dfrac{\omega\,z_j}{2\pi\tilde{U}_{z_j}(t_1)}\right]^{5/3}}}\\&\times\sqrt{\frac{1}{2}\frac{200}{2\pi}u_*^2(t_1)\frac{z_k}{\tilde{U}_{z_k}(t_1)}\frac{1}{\left[1+50\dfrac{\omega\,z_k}{2\pi\tilde{U}_{z_k}(t_1)}\right]^{5/3}}}\exp\left[-i\frac{\omega}{\pi}\frac{C_\theta(z_j-z_k)}{\tilde{U}_{z_k}(t_1)+\tilde{U}_{z_j}(t_1)}\right]\end{aligned} \tag{26}$$

Journal of Structural Engineering. Submitted December 15, 2011; accepted August 2, 2012;
posted ahead of print August 13, 2012. doi:10.1061/(ASCE)ST.1943-541X.0000697

For the non-stationary fluctuating wind velocity during the time $[0, T]$, its time-varying PSD function can be obtained when $\Delta t \to 0$. So, the time-varying PSD function is expressed as follows:

$$G_{z_j z_j}(\omega,t) = \frac{1}{2}\frac{200}{2\pi}u_*^2(t)\frac{z_j}{\tilde{U}_{z_j}(t)}\frac{1}{\left[1+50\dfrac{\omega\, z_j}{2\pi\tilde{U}_{z_j}(t)}\right]^{5/3}}$$
$$= \frac{1}{2}\frac{200}{2\pi}u_*^2(t)\frac{z_j}{U_{z_j}}\frac{1}{\left[1+50\dfrac{\omega\, z_j}{2\pi U_{z_j}}\right]^{5/3}}\frac{U_{z_j}}{\tilde{U}_{z_j}(t)}\left[\frac{1+50\dfrac{\omega\, z_j}{2\pi U_{z_j}}}{1+50\dfrac{\omega\, z_j}{2\pi\tilde{U}_{z_j}(t)}}\right]^{5/3} \quad (27)$$

Simultaneously, the time-varying cross PSD function can be determined using the following expression:

$$G_{z_j z_k}(\omega,t) = \Gamma(\omega,t)\sqrt{\left[G_{z_j z_j}(\omega,t)\right]\left[G_{z_k z_k}(\omega,t)\right]}\; e^{-i\theta_{jk}(\omega,\,t)}$$
$$= \exp\left[-\frac{\omega}{\pi}\frac{C_z|z_k - z_j|}{\tilde{U}_{z_j}(t)+\tilde{U}_{z_k}(t)}\right]\sqrt{\frac{1}{2}\frac{200}{2\pi}u_*^2(t)\frac{z_j}{\tilde{U}_{z_j}(t)}\frac{1}{\left[1+50\dfrac{\omega\, z_j}{2\pi\tilde{U}_{z_j}(t)}\right]^{5/3}}}$$
$$\times\sqrt{\frac{1}{2}\frac{200}{2\pi}u_*^2(t)\frac{z_k}{\tilde{U}_{z_k}(t)}\frac{1}{\left[1+50\dfrac{\omega\, z_k}{2\pi\tilde{U}_{z_k}(t)}\right]^{5/3}}}\;\exp\left[-i\frac{\omega}{\pi}\frac{C_\theta(z_j - z_k)}{\tilde{U}_{z_k}(t)+\tilde{U}_{z_j}(t)}\right] \quad (28)$$

Evidently, the non-stationary fluctuating wind velocity with both the time-varying PSD function and cross PSD function can be simulated with resorting to modulating stationary fluctuating wind velocity. In order to generate the non-stationary fluctuating wind velocity, an appropriate deterministic modulating function for modulating of the stationary fluctuating wind velocity with Kaimal spectrum will be derived in details in the next sub-section.

Journal of Structural Engineering. Submitted December 15, 2011; accepted August 2, 2012;
posted ahead of print August 13, 2012. doi:10.1061/(ASCE)ST.1943-541X.0000697

A proper deterministic modulating function

Based on the EPSD (Priestley 1967; Priestley 1988), the non-stationary stochastic process $u(t)$ with a zero-mean value admits the preceding Eq.(19), i.e.

$$u(t) = \int_{-\infty}^{+\infty} A(\omega,t)\, e^{i\omega t} d\, Z(\omega) \tag{29}$$

Likewise, $Z(\omega)$ satisfies

$$E\,[d\, Z(\omega)] = 0 \tag{30}$$

$$E[d\, Z^*(\omega_1)\, d\, Z(\omega_2)] = S(\omega_1)\, \delta(\omega_1 - \omega_2)\, d\omega_1\, d\omega_2 \tag{31}$$

in which $S(\omega)$ represents the PSD function of the corresponding stationary stochastic process.

Now, it is assumed that the fluctuating wind velocity is modeled as a non-stationary stochastic process and furthermore its PSD function of modulated stationary fluctuating wind velocity is in obedience to the Kaimal power spectrum. It follows that the EPSD function $G^0_{z_j z_j}(\omega,t)$ of the non-stationary fluctuating wind velocity can be expressed in the following form:

$$G^0_{z_j z_j}(\omega,t) = \left|A(\omega,t)\right|^2 S(\omega) = \left|A(\omega,t)\right|^2 \frac{1}{2}\frac{200}{2\pi} u_*^2 \frac{z_j}{U_{z_j}} \frac{1}{\left[1 + 50\dfrac{\omega\, z_j}{2\pi U_{z_j}}\right]^{5/3}} \tag{32}$$

Taking into account that $G^0_{z_j z_j}(\omega,t)$ in Eq.(32) is equivalent to $G_{z_j z_j}(\omega,t)$ in Eq.(27). Eq.(32) can be further recast in the following form:

Journal of Structural Engineering. Submitted December 15, 2011; accepted August 2, 2012;
posted ahead of print August 13, 2012. doi:10.1061/(ASCE)ST.1943-541X.0000697

$$
\begin{aligned}
G^{0}_{z_j z_j}(\omega,t) &= G_{z_j z_j}(\omega,t) \\
&= \frac{1}{2}\frac{200}{2\pi}u_*^2(t)\frac{z_j}{\tilde{U}_{z_j}(t)}\frac{1}{\left[1+50\dfrac{\omega\, z_j}{2\pi\tilde{U}_{z_j}(t)}\right]^{5/3}} \\
&= \frac{\tilde{U}_{z_j}(t)}{U_{z_j}}\left[\frac{1+50\dfrac{\omega\, z_j}{2\pi U_{z_j}}}{1+50\dfrac{\omega\, z_j}{2\pi\tilde{U}_{z_j}(t)}}\right]^{5/3}\frac{1}{2}\frac{200}{2\pi}u_*^2\frac{z_j}{U_{z_j}}\frac{1}{\left[1+50\dfrac{\omega\, z_j}{2\pi U_{z_j}}\right]^{5/3}} \\
&= \left|A(\omega,t)\right|^2 S(\omega)
\end{aligned}
\tag{33}
$$

It is known that the time-varying PSD being founded on a deterministic power spectrum can be represented by EPSD. Hence, we derive that

$$
A(\omega,t) = \sqrt{\frac{\tilde{U}_{z_j}(t)}{U_{z_j}}\left[\frac{1+50\dfrac{\omega\, z_j}{2\pi U_{z_j}}}{1+50\dfrac{\omega\, z_j}{2\pi\tilde{U}_{z_j}(t)}}\right]^{5/3}}
\tag{34}
$$

Likewise, for other power spectra such as *Davenport*, *Harris* and *Simiu*, the corresponding deterministic modulating functions can be derived in the same way, and they have been listed in Table 1.

Based on Kaimal power spectrum, the evolutionary cross power spectrum density (ECPSD) function $G^{0}_{z_j z_k}(\omega,t)$ can be derived through a deterministic modulating function as Equation (34).

Journal of Structural Engineering. Submitted December 15, 2011; accepted August 2, 2012; posted ahead of print August 13, 2012. doi:10.1061/(ASCE)ST.1943-541X.0000697

$$G^{0}_{z_j z_k}(\omega,t) = A_j(\omega,t)\,A_k(\omega,t)\sqrt{\left[S_j(\omega)\right]\left[S_k(\omega)\right]}\;\Gamma(\omega,t)\;e^{-i\theta_{jk}(\omega,\,t)}$$

$$\begin{aligned}
&= \sqrt{\frac{\tilde{U}_{z_j}(t)}{U_{z_j}}\left[\frac{1+50\dfrac{\omega\, z_j}{2\pi U_{z_j}}}{1+50\dfrac{\omega\, z_j}{2\pi \tilde{U}_{z_j}(t)}}\right]^{5/3}}\sqrt{\frac{\tilde{U}_{z_k}(t)}{U_{z_k}}\left[\frac{1+50\dfrac{\omega\, z_k}{2\pi U_{z_k}}}{1+50\dfrac{\omega\, z_k}{2\pi \tilde{U}_{z_k}(t)}}\right]^{5/3}} \\
&\times \sqrt{\frac{1}{2}\frac{200}{2\pi}u_*^2\frac{z_j}{U_{z_j}}\frac{1}{\left[1+50\dfrac{\omega\, z_j}{2\pi U_{z_j}}\right]^{5/3}}}\sqrt{\frac{1}{2}\frac{200}{2\pi}u_*^2\frac{z_k}{U_{z_k}}\frac{1}{\left[1+50\dfrac{\omega\, z_k}{2\pi U_{z_k}}\right]^{5/3}}} \\
&\times \exp\left[-\frac{\omega}{\pi}\frac{C_z\left|z_k-z_j\right|}{\tilde{U}_{z_j}(t)+\tilde{U}_{z_k}(t)}\right]\exp\left[-i\frac{\omega}{\pi}\frac{C_\theta(z_j-z_k)}{\tilde{U}_{z_k}(t)+\tilde{U}_{z_j}(t)}\right] \\
&= \exp\left[-\frac{\omega}{\pi}\frac{C_z\left|z_k-z_j\right|}{\tilde{U}_{z_j}(t)+\tilde{U}_{z_k}(t)}\right]\sqrt{\frac{1}{2}\frac{200}{2\pi}u_*^2\frac{z_j}{\tilde{U}_{z_j}(t)}\frac{1}{\left[1+50\dfrac{\omega\, z_j}{2\pi \tilde{U}_{z_j}(t)}\right]^{5/3}}} \\
&\times \sqrt{\frac{1}{2}\frac{200}{2\pi}u_*^2\frac{z_k}{\tilde{U}_{z_k}(t)}\frac{1}{\left[1+50\dfrac{\omega\, z_k}{2\pi \tilde{U}_{z_k}(t)}\right]^{5/3}}}\exp\left[-i\frac{\omega}{\pi}\frac{C_\theta(z_j-z_k)}{\tilde{U}_{z_k}(t)+\tilde{U}_{z_j}(t)}\right]
\end{aligned} \tag{35}$$

Seeing that Eq.(35) is equivalent to Eq.(28), the ECPSD function $G^{0}_{z_j z_k}(\omega,t)$ is also equal to the time-varying cross PSD function $G_{z_j z_k}(\omega,t)$. So, the derivation of deterministic modulating function is effective for the modulation of stationary fluctuating wind velocities.

Application of the proposed technique

The aim of this section is to numerically simulate the non-stationary fluctuating wind velocity time series at three dissimilar points 1, 2, and 3 envisaged, shown in Figure 1, with resorting to the derived deterministic modulating function above. Likewise, the SIA is introduced into the SR method for reducing the number of the Cholesky decomposition of power spectral matrix. The variables $u_1(t)$, $u_2(t)$, $u_3(t)$ are, respectively, employed to represent the three components

Journal of Structural Engineering. Submitted December 15, 2011; accepted August 2, 2012;
posted ahead of print August 13, 2012. doi:10.1061/(ASCE)ST.1943-541X.0000697

of this one-dimensional trivariate stochastic process. Kaimal power spectrum and corresponding modulating function listed in Table 1 are taken into consideration herein. It is hypothesized that the time-varying mean wind velocity at the first point 1 (height $z = 35\ m$) satisfies $\tilde{U}_{35} = U_{35}\ [1 + \gamma \cos(\omega' t)] = 45\ [1 + 0.3\cos(0.0052t)]\ m/s$. It is worth pointing out that the time-varying mean wind speed can be also generated by using a sequence of independent random numbers from normal distribution and Weibull distribution (Aksoy *et al*. 2004; Torrielli *et al*. 2011). For the downburst, the time-varying mean wind speed, namely the non-turbulent wind velocity of downburst can be simulated by empirical model or analytical model (Chen and Letchford 2004; Chay *et al*. 2006). Likewise, the surface rough roughness length is taken as $z_0 = 0.001266\,m$, which corresponds to the shear velocity of the flow $u_* = 1.76\,m/s$. It is pointed herein out that the values $z_0 = 0.001266\,m$ and $u_* = 1.76\,m/s$ are taken from Simiu and Scanlan (1986). Then, the time-varying mean wind velocities at the second and third points are calculated in terms of $\tilde{U}_{45} = 46.1\,[1 + 0.3\cos(0.0052t)]$ and $\tilde{U}_{145} = 51.3\,[1 + 0.3\cos(0.0052t)]$, respectively. In the present simulation, the upper cutoff circle frequency is set equal to be $\omega_{up} = 4\ \ rad/s$, the dividing number of circle frequency is selected to be $N = 2048$, and $\Delta t = 0.785s$ is the time step of numerical simulation with a time length equal to $T = 3216.99s$. By resorting to the short-time Fourier transform (STFT), the EPSD function can be estimated from the generated non-stationary fluctuating wind velocity by using the proposed method. The STFT, $F(\omega, t)$, of stochastic process, $u(t)$, is defined by the convolution integral below.

$$G(\omega, t) = \int_{-\infty}^{+\infty} u(\tau)\ h(t - \tau)\ e^{-i\omega\tau}\ d\tau \tag{36}$$

In the preceding equation, $h(t)$ represents an appropriate time window. In the present

Journal of Structural Engineering. Submitted December 15, 2011; accepted August 2, 2012;
posted ahead of print August 13, 2012. doi:10.1061/(ASCE)ST.1943-541X.0000697

paper, the time window squared function is selected to be $h^2(t)=\frac{1}{\sqrt{2\pi}\sigma}e^{-t^2/2\sigma^2}$ $(\sigma=0.25)$. The square of the module for the EPSD function, namely $G(\omega,t)$, can then be explicitly written as follows:

$$\left|F(\omega,t)\right|^2=\int_{-\infty}^{+\infty}\int_{-\infty}^{+\infty}u(\tau_1)\,u(\tau_2)\,h(t-\tau_1)\,h(t-\tau_2)e^{-i\omega\tau_1}\,e^{-i\omega\tau_2}\,d\tau \tag{37}$$

In fact, to estimate EPSD function, there are a number of methods. For example, it is also a good choice to adopt wavelet, which is studied as a more advanced approach to estimate EPSD functions of non-stationary stochastic processes (Spanos and Failla 2004; Spanos *et al*. 2005).

Figure 2 [including (a), (b), and (c)] displays the sample functions of longitudinal non-stationary fluctuating wind velocities at three dissimilar points 1, 2, and 3 generated by using the present method. In order to better visualize the differences and the similarities among these three time histories, Figure 3 presents the enlarged views of the initial 600s of simulated sample functions displayed in Figure 2. As far as the degree of correlation among these three time histories is concerned, Figure 3 clearly demonstrates that with the decreasing of the distance between arbitrary two points, the loss of coherence between two samples, corresponding respectively to these two points, takes on a decreasing trend. For example, since the distance between the points 1 and 2 is only 10 m apart, there is a small loss of coherence between $u_1(t)$ and $u_2(t)$. On the other hand, there exists a considerable loss of coherence between $u_1(t)$ and $u_3(t)$ and between $u_2(t)$ and $u_3(t)$, as the point 3 is located at 110m from the point 1 and 100m from the point 2 (see Figure 1). The coherence between the generated wind fluctuations weakens along with the distance increases. Evidently, this

Journal of Structural Engineering. Submitted December 15, 2011; accepted August 2, 2012;
posted ahead of print August 13, 2012. doi:10.1061/(ASCE)ST.1943-541X.0000697

phenomenon is controlled by the coherence function. Simultaneously, it can be clearly detected from Figure 3 that there exists a phase angle between arbitrary two samples at the 100s time instant. Figures 4 and 5, respectively, provide both the temporal auto-correlation and cross-correlation functions of the generated sample functions displayed in Figure 2 with respect to the corresponding targets at the time instant $t = 100.53s$. Figures 4 and 5 clearly demonstrate that the simulated $R_{jk}(t,t+\tau)$ is in reasonable agreement with the target, $R^{0}_{jk}(t,t+\tau)$, while admitting that there exists a small degree of differences. Further, these differences tend to disappear when the auto- and cross-correlation functions, $R_{jk}(t,t+\tau)$ is computed in terms of the 20000 sample functions at the time instant $t = 100.53s$. Under this scenario, the simulated $R_{jk}(t,t+\tau)$ is in remarkable agreement with the target, $R^{0}_{jk}(t,t+\tau)$. Additionally, it can be detected from Figure 5 that the peak values of auto- and cross-correlation functions exhibit the time shift. This phenomenon embodies that the sample possesses the phase difference. Finally, by means of the STFT, the EPSD function, $G(\omega,t)$, is estimated from these sample time histories and plotted in Figure 6. Indubitably, the simulated EPSD functions possess the time-varying features. Therefore, the present procedure is capable of fully capturing the non-stationarity. Moreover, Figure 7 presents the EPSD functions of the generated sample functions displayed in figure 2 with reference to the corresponding targets at the time instant $t = 100.53s$. It is seen from Figure 7 that the EPSD functions, $G(\omega,t_1)$, are generally in agreement with the targets at the time instant $t_1 = 100.53s$.

In order to demonstrate the superiority of introducing SIA into SR method (the SSR method) in enhancing the computational efficiency of generating non-stationary stochastic

Journal of Structural Engineering. Submitted December 15, 2011; accepted August 2, 2012;
posted ahead of print August 13, 2012. doi:10.1061/(ASCE)ST.1943-541X.0000697

processes, the dividing number of circle frequency $N = 4096,\ 8192$ and the length of simulation time $T = 4823.04s,\ 6430.72s$ are also taken into consideration. The Cholesky decomposition in the SSR method is implemented on only 128 circular frequency points at each instant of simulation. The comparisons among several different schemes are made and listed in Table 2. It can be seen from Case 1 in Table 2, the elapsed time for the simulation with SR is 347*s*, while that for the simulation with SSR is only 58*s*. The time consumption of SSR reduces more than 80% the elapsed time of SR. Along with the increasing of the length of simulation time, the proportion of the elapsed time between SSR and SSR keeps about 17% as seen from Case1 to Case 3. Apparently, in the calculation speed the SSR has considerable advantage over the SR. Furthermore, the superiority becomes more remarkable with the increasing of *N*. For example, in Case 5, the elapsed time of SSR is 8.9% of the time consumption of SR, and the percentage is the smallest in these cases. This is because, the number of the Cholesky decomposition in the SSR method keeps constant with the value equal to 128 at each instant of simulation, but in the SR method the decomposition number is also more and more as *N* increases. Therefore, introducing SIA into SR method is able to enhance the computational efficiency of simulating non-stationary stochastic processes.

It is noted that the above-mentioned fluctuating wind speeds shown in Figure 2 take on weak non-stationarities. The main reason may be that the time-varying mean wind speed of the modulating function is slowly time-varying function with small-amplitude and long-period. For simulating strong non-stationarity, the turbulent wind velocity of downburst is taken into account. As displayed in Figure 8, the modified OBV model (Chay *et al.* 2006) is considered as

Journal of Structural Engineering. Submitted December 15, 2011; accepted August 2, 2012;
posted ahead of print August 13, 2012. doi:10.1061/(ASCE)ST.1943-541X.0000697

the non-turbulent wind velocity of downburst, namely the time-varying mean wind speed. In like manner, Kaimal power spectrum and corresponding modulating function listed in Table 1 are also taken into consideration herein. Figure 9 presents the generated downburst, and Figure 10 displays the simulated turbulent wind velocity which takes on strong non-stationarity. The non-stationarity is relevant to the modulating function. It can be seen from Figure 10 that the amplitude of fluctuating wind speed is bigger when the non-turbulent wind velocity of downburst is greater, which is consistent with what expressed by the Equation (34). By means of the STFT, the EPSD function is also estimated from the simulated turbulent wind velocity of downburst and plotted in Figure 11. Undoubtedly, the simulated EPSD function possesses the time-varying features.

6. Conclusions

Nowadays, most simulations of the non-stationary stochastic processes have been developed around the reproduction of earthquake ground motions known to be highly non-stationary. In the present paper, instead, generation of the non-stationary fluctuating wind velocity has been addressed. Non-stationarity is achieved by modulating the stationary fluctuating wind velocity.

The present study proposes an effective approach to obtain appropriate deterministic modulating function enabled to modulate non-uniformly stationary fluctuating wind velocity, which is believed to be new in the literature. By means of derivation, a deterministic modulating function is deduced in detail according to the Kaimal power spectrum. Likewise, other

Journal of Structural Engineering. Submitted December 15, 2011; accepted August 2, 2012;
posted ahead of print August 13, 2012. doi:10.1061/(ASCE)ST.1943-541X.0000697

deterministic modulating functions can be also derived based on different power spectra, such as Davenport power spectrum, Harris power spectrum, Simiu power spectrum and so on. On the other hand, when digitally simulating the non-stationary stochastic processes through the SR method, there is a need for reducing the increasing number of the Cholesky decomposition of the time-varying spectral density matrix. Distinguished from the FFT algorithm, the SIA can be used when the modulating function is a deterministic time-frequency function. Thus, the SIA is taken into account and thereupon introduced into the SR method so as to decrease the Cholesky decomposition of the time-varying spectral density matrix. An example application to reproducing the non-stationary fluctuating wind velocity time series at three dissimilar points envisaged is described in detail. Results confirm the effectiveness and faithfulness of the simulated non-stationary stochastic processes, and show that the derived modulating function can capture fully the nonstationarity of wind velocities. Finally, based on the proposed technique, the turbulent wind velocity of downburst is generated to simulate the strong non-stationarity.

The aforesaid elucidation demonstrates that the present procedure can generate a library of non-stationary fluctuating wind velocity for use in wind-resistant analysis and design.

Acknowledgements

The author would like to acknowledge the financial contributions received from the National Science Foundation of China with Grant No.11162005 and National Science Foundation of China with Grant No.51068005. The author wishes to thank the reviewers for their careful,

Journal of Structural Engineering. Submitted December 15, 2011; accepted August 2, 2012;
posted ahead of print August 13, 2012. doi:10.1061/(ASCE)ST.1943-541X.0000697

unbiased, and constructive suggestions, which significantly improved the quality of this paper.

References

Aksoy, H., Fuat Toprak, Z., Aytek, A., and Erdem Ünal, N. (2004). "Stochastic generation of hourly mean wind speed data." *Renew. Energy.*, 29, 2111-2131.

Chay, M.T., Albermani, F., and Wison, R. (2006). "Numerical and analytical simulation of downburst wind loads." *Eng. Struct.*, 28, 240-254.

Chen, L., and Letchford, C.W. (2004). "A deterministic-stochastic hybrid model of downbursts and its impact on a cantilevered structure." *Eng. Struct.*, 26, 619-629

Chen, L., and Letchford, C.W. (2005a). "Simulation of Multivariate Stationary Gaussian Stochastic Processes: Hybrid Spectral Representation and Proper Orthogonal Decomposition Approach." *J. Eng. Mech.*, 131(8), 801-808.

Chen, L., and Letchford, C.W. (2005b). "Proper orthogonal decomposition of two vertical profiles of full-scale nonstationary downburst wind speed." *J. Wind Eng. Ind. Aerodyn.*, 93(3), 187-216.

Chen, L., and Letchford, C.W. (2007). "Numerical simulation of extreme winds from thunderstorm downbursts." *J. Wind Eng. Ind. Aerodyn.*, 95(9-11), 977-990.

Chen, Z.X. (2008). "Analysis of alongwind tall building response to transient nonstationary winds." *J. Struct. Eng.*, 134(5), 782-791.

Cramer, H., and Leadbetter, M.R. (1967). *Stationary and related stochastic processes*. John Wiley, New York.

Journal of Structural Engineering. Submitted December 15, 2011; accepted August 2, 2012; posted ahead of print August 13, 2012. doi:10.1061/(ASCE)ST.1943-541X.0000697

Davenport, A.G. (1967). "The dependence of wind load upon meteorological parameters." *Proceedings of Symposium on Wind Effects on Buildings and Structure*, University of Toronto Press, Ottawa, 1, 19-82.

Di Paola, M. (1998). "Digital simulation of wind field velocity." *J. Wind Eng. Ind. Aerodyn.*, 74-76, 91-109.

Deodatis, G. (1996). "Nonstationary stochastic vector processes: Seismic ground motion applications." *Prob. Eng. Mech.*, 11(3), 149-168.

Deodatis, G. (1996). "Simulation of ergodic multivariate stochastic processes." *J. Eng. Mech.*, 122(8), 778-787.

Der Kiureghian, A, and Crempien, J. (1989). "An evolutionary model for earthquake ground motion." *Struct. Saf.*, 6, 235-246.

Grigoriu, M. (1993). "On the spectral representation method in simulation." *Prob. Eng. Mech.*, 8, 75-90.

Grigoriu, M., Ruiz, S.E., and Rosenblueth. E. (1988). "Nonstationary models of seismic ground acceleration." *Technical Rep. NCEER-88-0043*, National Center for Earthquake Engineering Research, Buffalo, NY.

Kaimal, J.C., Wyngaard, J.C., Izumi, Y., and Cote, O.R. (1972). "Spectral characteristics of surface-layer turbulence." *J. Roy. Meteor. Soc.*, 98, 563-589.

Kareem, A. (2008). "Numerical simulation of wind effects: A probabilistic perspective." *J. Wind Eng. Ind. Aerodyn.*, 96, 1472-1497.

Kareem, A., and Li, Y. (1992). "Digital simulation of wind load effects." *Proc., ASCE Specialty*

Conf. on Probabilistic Mechanics and Structural and Geotechnical Reliability, ASCE, Reston, VA, 284-287.

Kozin, F. (1988). "Autoregressive moving-average models of earthquake records." *Prob. Eng. Mech.*, 3(2), 58-63.

Kristensen, L., and Jensen, N.O. (1979). "Lateral coherence in isotropic turbulence and in the natural wind." *Bound-Lay. Meteorol*., 17, 353-373.

Lawson, T.V. (1980). *Wind effects on buildings: Statistics and meteorology-Part II*. Applied Science, London.

Li, C.X., and Li, J.H. (2011). "Simulation of non-Gaussian random field for boundary in-plane imperfection." *Adv. Sci. Lett.*, 4(3):943-947.

Li, C.X., and Li, J.H. (2012). "Support vector machines approach to conditional simulation of non-Gaussian stochastic process." *J. Comput. Civil Eng.,* 2012, 26(1):131-140.

Li, J.H., and Li, C.X. (2012). "Simulation of non-Gaussian stochastic process with target power spectral density and lower-order moments." *J. Eng. Mech.,* 138(5):391-404.

Li. J.H., Li, C.X., and Chen, S.S. (2011). "Spline-interpolation-based FFT Approach to Fast Simulation of Multivariate Stochastic Processes." *Math. Probl. Eng.*, Volume 2011, Article ID 842183, 24 pages, doi:10.1155/2011/842183.

Li, Y., and Kareem, A. (1991). "Simulation of multivariate nonstationary random processes by FFT." *J. Eng. Mech.*, 117, 1037-1058.

Li, Y., and Kareem, A. (1997). "Simulation of multivariate nonstationary random processes: hybrid DFT and digital filtering approach." *J. Eng. Mech.*, 123(12), 1302-1310.

Journal of Structural Engineering. Submitted December 15, 2011; accepted August 2, 2012; posted ahead of print August 13, 2012. doi:10.1061/(ASCE)ST.1943-541X.0000697

Liang, J.W., Chaudhuri, S.R., and Shinozuka, M. (2007). "Simulation of nonstationary stochastic processes by spectral representation." *J. Eng. Mech.*, 133(6), 616-627.

Mignolet, M.P., and Spanos, P.D. (1990). "MA to ARMA modeling of wind." *J. Wind Eng. Ind. Aerodyn.*, 36(1-3), 429-438.

Mignolet, M.P., and Spanos, P.D. (1992). "Simulation of Homogeneous Two-Dimensional Random Fields: Part I---AR and ARMA Models." *J. Appl. Mech.*, 59(2S), 260-269.

Novak, D., Stoyanoff, S., and Herda, H. (1995). "Error assessment for wind histories generated by autoregressive method." *Struct. Saf.*, 17(2), 79-90.

Peil, U., and Telljohann, G. (1996). "Lateral turbulence and dynamic response." *Struct. Dynamics*, 1(5-8), 207-211.

Priestley, M.B. (1965). "Evolutionary spectra and non-stationary processes." *J. Roy. Stat. Soc. B.*, 27, 204-237.

Priestley, M.B. (1967). "Power spectral analysis of non-stationary random processes." *J. Sound Vib.*, 6, 86-97.

Priestley, M.B. (1988). *Non-linear and non-stationary time series analysis*. Academic Press, London.

Rossi, R., Lazzari, M., and Vitaliani, R. (2004). "Wind field simulation for structural engineering purposes." *Int. J. Numer. Meth. Eng.*, 61, 738-763.

Saragoni, G.R., and Hart, G.C. (1973). "Simulation of artificial earthquakes." *Earthq. Eng. Struct. Dyn.*, 2(3), 249-267.

Shinozuka, M., and Deodatis, G. (1991). "Simulation of stochastic processes by spectral

Journal of Structural Engineering. Submitted December 15, 2011; accepted August 2, 2012; posted ahead of print August 13, 2012. doi:10.1061/(ASCE)ST.1943-541X.0000697

representation." *Appl. Mech. Rev.*, 44, 191-204.

Simiu, E., and Scanlan, R.H. (1986). *Wind effects on structures*. John Wiley, New York.

Spanos, P.D., and Failla, G. (2004). "Evolutionary spectra estimation using wavelets." *J. Eng. Mech.*, 130(8), 952-960.

Spanos, P.D., and Mignolet, M.P. (1987). "Recursive simulation of stationary multivariate random processes-Part II." *J. Appl. Mech.*, 54(3), 681-687.

Spanos, P.D., and Mignolet, M.P. (1990). "Simulation of stationary random processes: two stage MA to ARMA approach." *J. Eng. Mech.*, 116(3), 620-641.

Spanos, P.D., and Mignolet, M.P. (1992). "Simulation of Homogeneous Two-Dimensional Random Fields: Part II---MA and ARMA Models." *J. Appl. Mech*., 59(2S): 270-277.

Spanos, P.D., Tezcan, J., and Tratskas, P. (2005). "Stochastic processes evolutionary spectrum estimation via harmonic wavelets." *Comput. Methods Appl. Mech. Engrg*., 194, 1367-1383.

Torrielli, A., Repetto, M.P., and Solari, G. (2011). "Long-term simulation of the mean wind speed." *J. Wind Eng. Ind. Aerodyn*., 99, 1139-1150.

Wang, L., and Kareem, A. (2004). "Modeling of non-stationary winds in gust fronts." *Proceedings of the 9th ASCE Specialty Conference on Probabilistic Mechanics and Structural Reliability*, PMC2004, Albuquerque, New Mexico, 26-28.

Wang, L., and Kareem, A. (2005). "Modeling and simulation of transient winds: downbursts / hurricanes." *Proceedings of the 10th American Conference on Wind Engineering*, AAWE, Louisiana State University.

Wittig, L.E., and Sinhat, A.K. (1975). "Simulation of multicorrelated random processes using

Journal of Structural Engineering. Submitted December 15, 2011; accepted August 2, 2012;
posted ahead of print August 13, 2012. doi:10.1061/(ASCE)ST.1943-541X.0000697

the FFT Algorithm." *J. Acoust. Soc. Am.*, 58(3), 630-634.

Xu, Y.L., and Chen, J. (2004). "Characterizing nonstationary wind speed using empirical mode decomposition." *J. Struct. Eng.*, 130(6), 912–920.

Yang, J.N. (1972). "Simulation of random envelope process." *J. Sound Vib.*, 25(1), 73-85.

Yang, J.N. (1973). "On the normality and accuracy of simulated random processes." *J. Sound Vib.*, 26(3), 417-428.

Yeh, C.H., and Wen, Y.K. (1990). "Modeling of nonstationary ground motion and analysis of inelastic structural response." *Struct. Saf.*, 8, 281-298.

Journal of Structural Engineering. Submitted December 15, 2011; accepted August 2, 2012;
posted ahead of print August 13, 2012. doi:10.1061/(ASCE)ST.1943-541X.0000697

Figure captions list

Fig.1 Locations of points 1, 2, and 3 along a vertical line.

Fig.2 The generated sample functions for longitudinal non-stationary fluctuating wind velocities at three different heights.

Fig.3 Enlarged views of the initial 600s of the simulated sample functions for longitudinal non-stationary fluctuating wind velocities at three different heights, displayed in Fig. 2.

Fig. 4. Temporal auto-correlation functions of the generated sample functions displayed in Fig. 2 with respect to the corresponding targets at the time instant $t = 100.53s$.

Fig. 5. Temporal cross-correlation functions of the generated sample functions displayed in Fig. 2 with reference to the corresponding targets at the time instant $t = 100.53s$.

Fig. 6. EPSD functions of the generated sample functions displayed in Fig. 2.

Fig. 7. EPSD functions of the generated sample functions displayed in Fig. 2 with regard to the corresponding targets at the time instant $t = 100.53s$.

Fig. 8. The time-varying mean wind speed of downburst generated using the modified OBV model.

Journal of Structural Engineering. Submitted December 15, 2011; accepted August 2, 2012;
posted ahead of print August 13, 2012. doi:10.1061/(ASCE)ST.1943-541X.0000697

Fig. 9. Wind speed time history of the generated downburst

Fig. 10. Turbulent wind speed time history of the generated downburst

Fig. 11. EPSD function of the generated turbulent wind speed displayed in Fig. 10

Figure 1

Journal of Structural Engineering. Submitted December 15, 2011; accepted August 2, 2012;
posted ahead of print August 13, 2012. doi:10.1061/(ASCE)ST.1943-541X.0000697

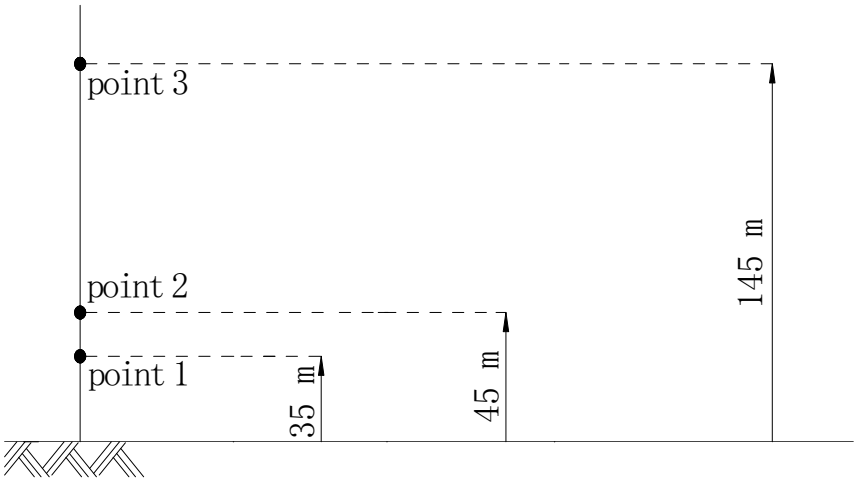

Fig. 1. Locations of points 1, 2, and 3 along a vertical line.

Figure 2

Journal of Structural Engineering. Submitted December 15, 2011; accepted August 2, 2012;
posted ahead of print August 13, 2012. doi:10.1061/(ASCE)ST.1943-541X.0000697

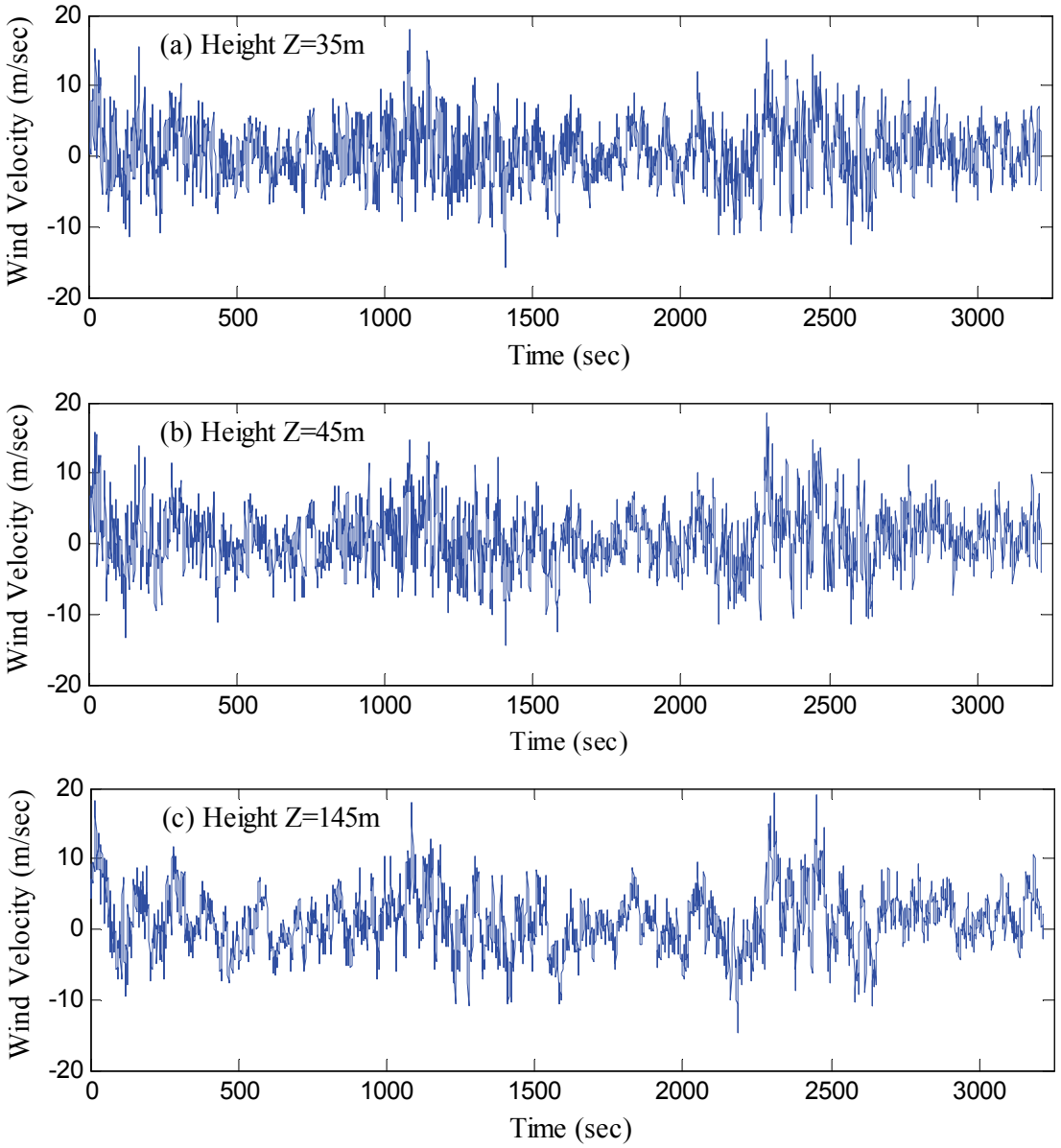

Fig. 2. The generated sample functions for longitudinal non-stationary fluctuating wind velocities at three different heights.

Figure 3

Journal of Structural Engineering. Submitted December 15, 2011; accepted August 2, 2012;
posted ahead of print August 13, 2012. doi:10.1061/(ASCE)ST.1943-541X.0000697

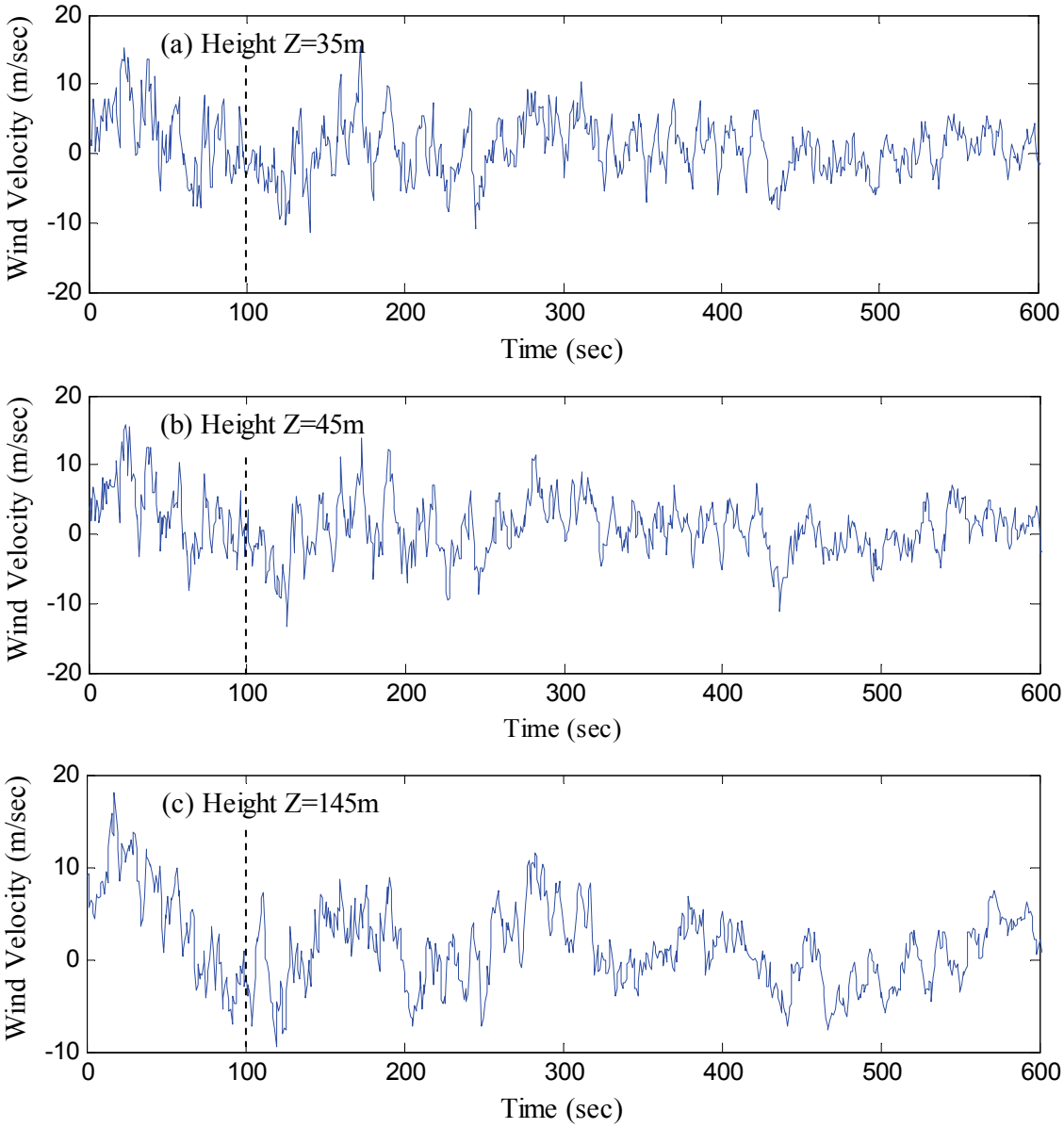

Fig. 3. Enlarged views of the initial 600s of the simulated sample functions for longitudinal non-stationary fluctuating wind velocities at three different heights, displayed in Fig. 2.

Figure 4

Journal of Structural Engineering. Submitted December 15, 2011; accepted August 2, 2012;
posted ahead of print August 13, 2012. doi:10.1061/(ASCE)ST.1943-541X.0000697

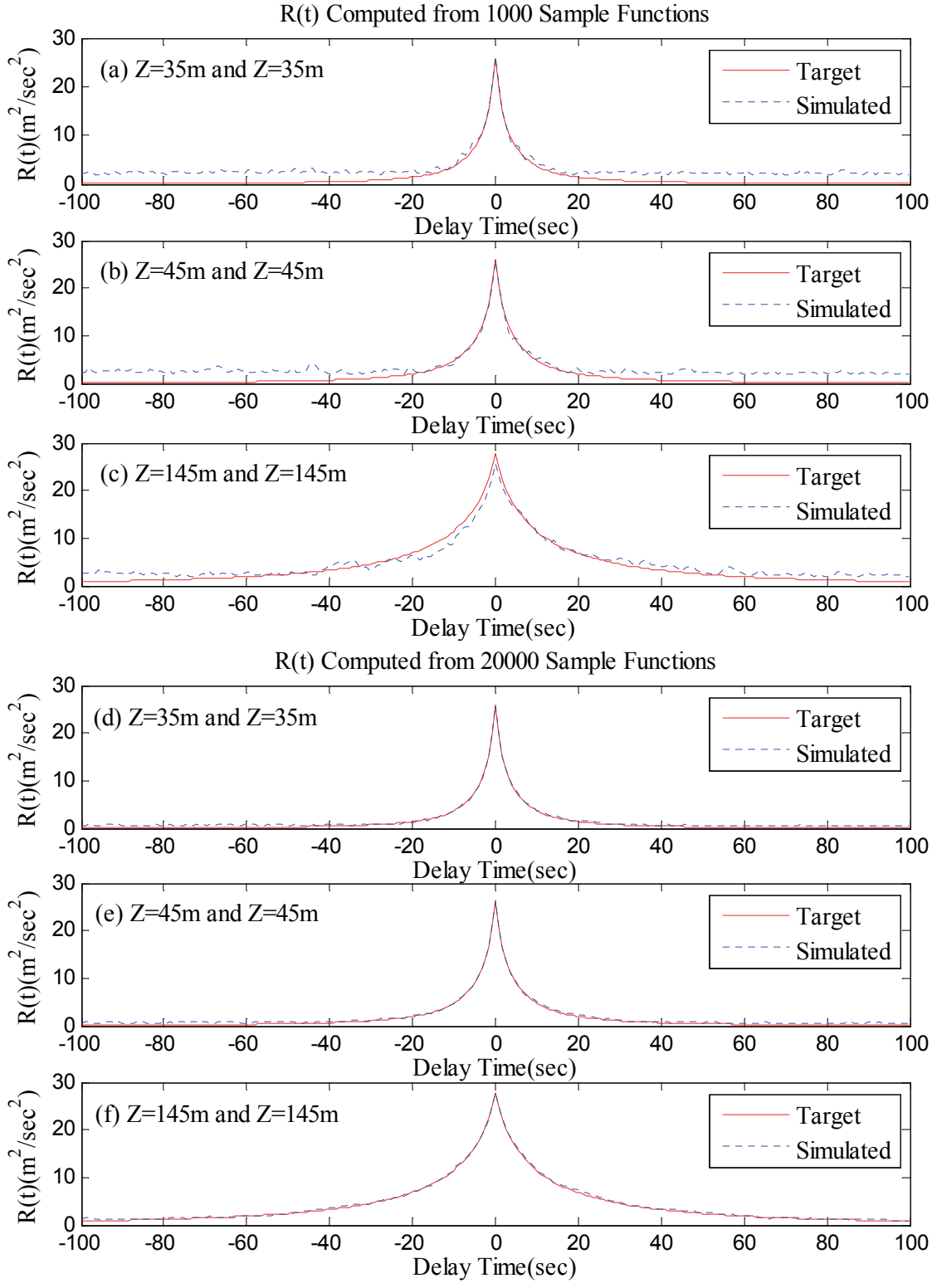

Fig. 4. Temporal auto-correlation functions of the generated sample functions displayed in Fig. 2 with respect to the corresponding targets at the time instant $t = 100.53s$.

Figure 5

Journal of Structural Engineering. Submitted December 15, 2011; accepted August 2, 2012;
posted ahead of print August 13, 2012. doi:10.1061/(ASCE)ST.1943-541X.0000697

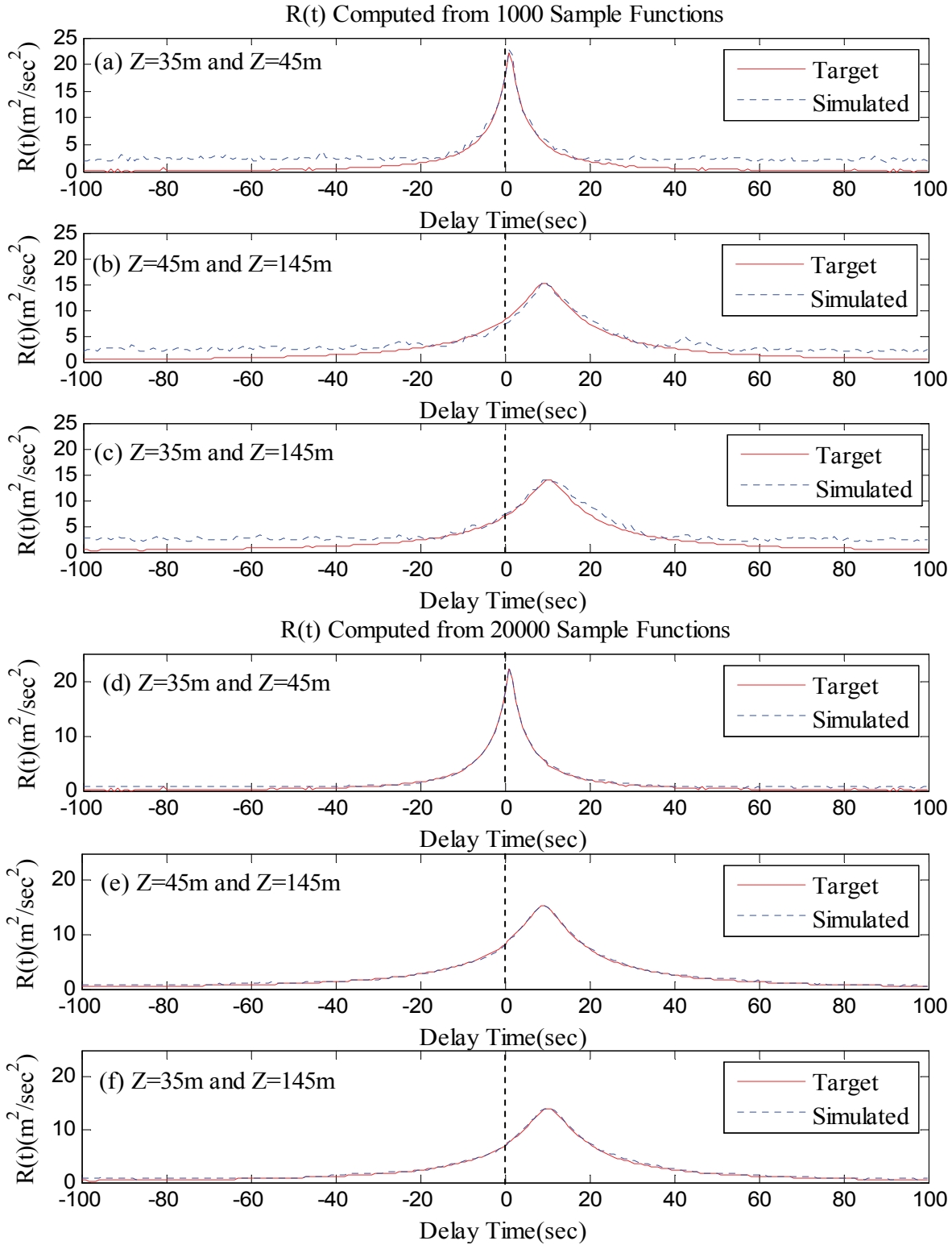

Fig. 5. Temporal cross-correlation functions of the generated sample functions displayed in Fig. 2 with reference to the corresponding targets at the time instant $t = 100.53s$.

Figure 6

Journal of Structural Engineering. Submitted December 15, 2011; accepted August 2, 2012;
posted ahead of print August 13, 2012. doi:10.1061/(ASCE)ST.1943-541X.0000697

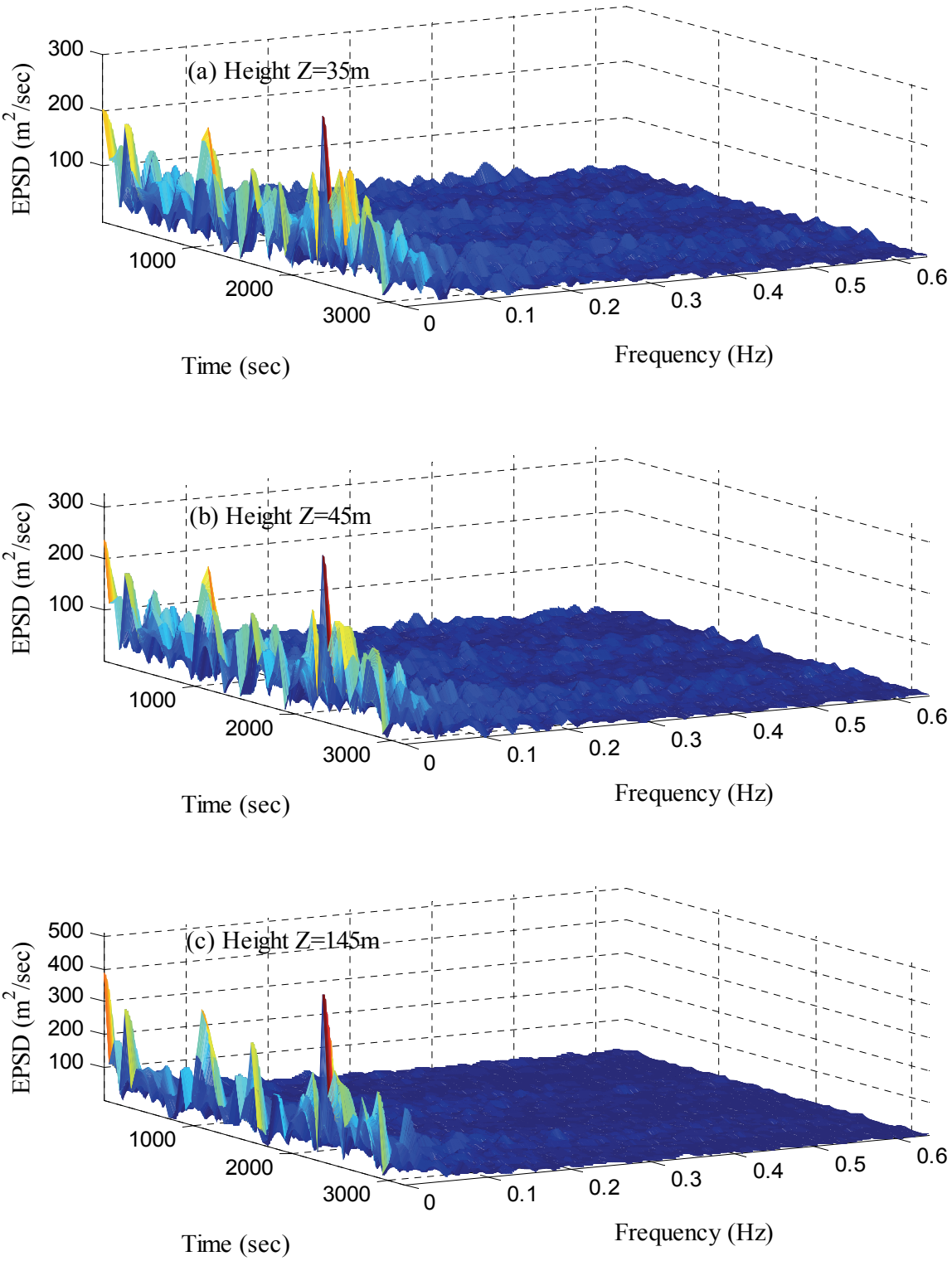

Fig. 6. EPSD functions of the generated sample functions displayed in Fig. 2.

Figure 7

Journal of Structural Engineering. Submitted December 15, 2011; accepted August 2, 2012;
posted ahead of print August 13, 2012. doi:10.1061/(ASCE)ST.1943-541X.0000697

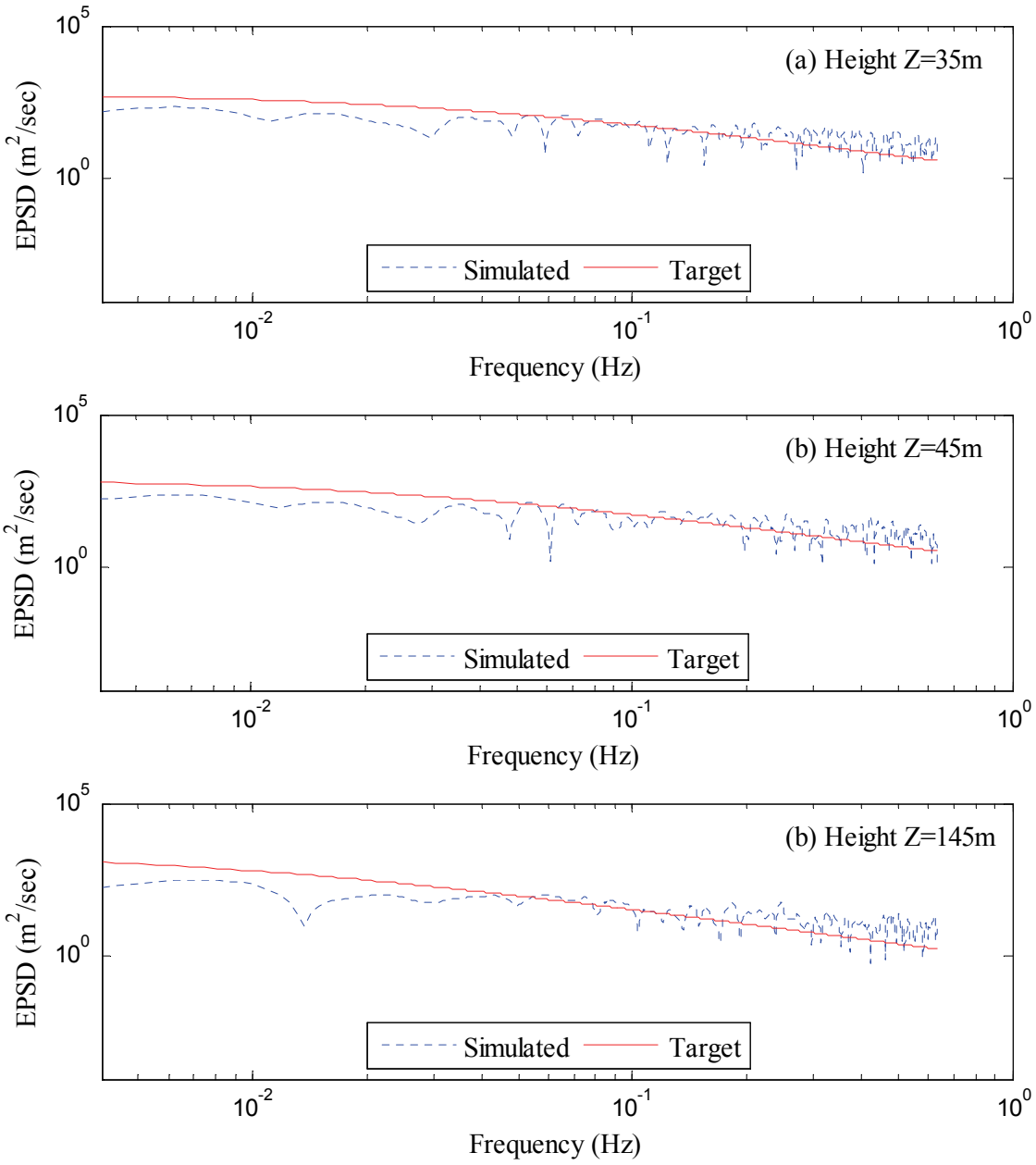

Fig. 7. EPSD functions of the generated sample functions displayed in Fig. 2 with regard to the corresponding targets at the time instant $t = 100.53s$.

Figure 8

Journal of Structural Engineering. Submitted December 15, 2011; accepted August 2, 2012;
posted ahead of print August 13, 2012. doi:10.1061/(ASCE)ST.1943-541X.0000697

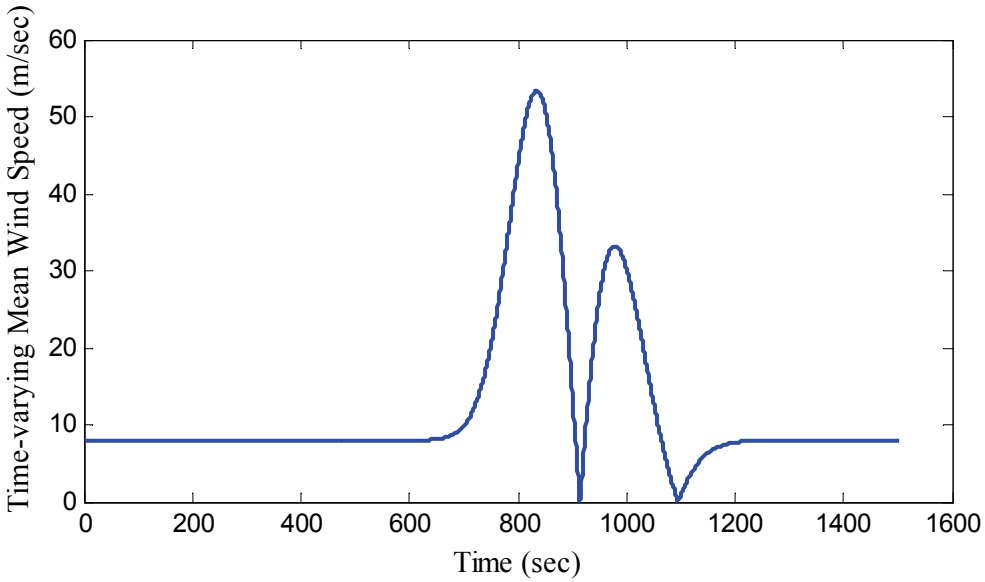

Fig. 8. The time-varying mean wind speed of downburst generated using the modified OBV model.

Figure 9

Journal of Structural Engineering. Submitted December 15, 2011; accepted August 2, 2012;
posted ahead of print August 13, 2012. doi:10.1061/(ASCE)ST.1943-541X.0000697

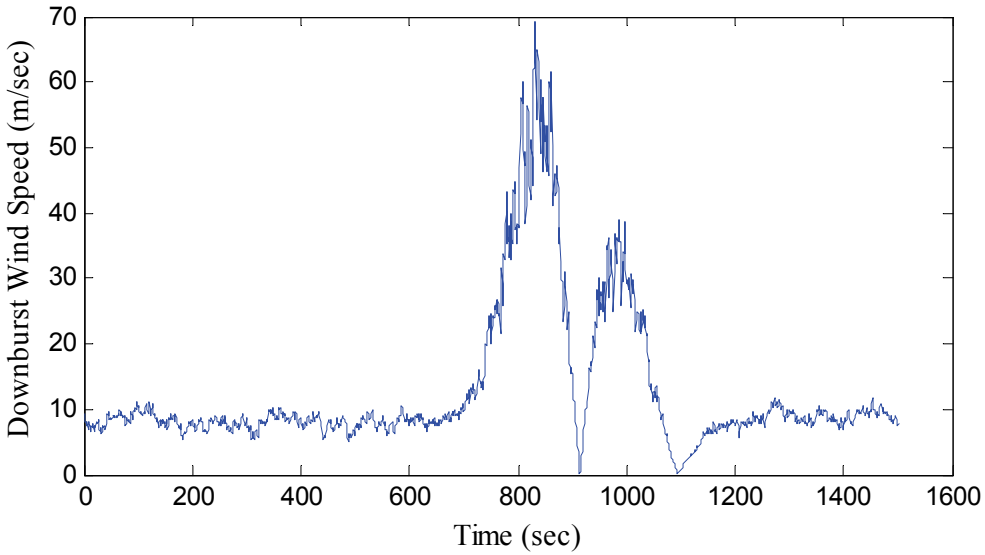

Fig. 9. Wind speed time history of the generated downburst

Figure 10

Journal of Structural Engineering. Submitted December 15, 2011; accepted August 2, 2012;
posted ahead of print August 13, 2012. doi:10.1061/(ASCE)ST.1943-541X.0000697

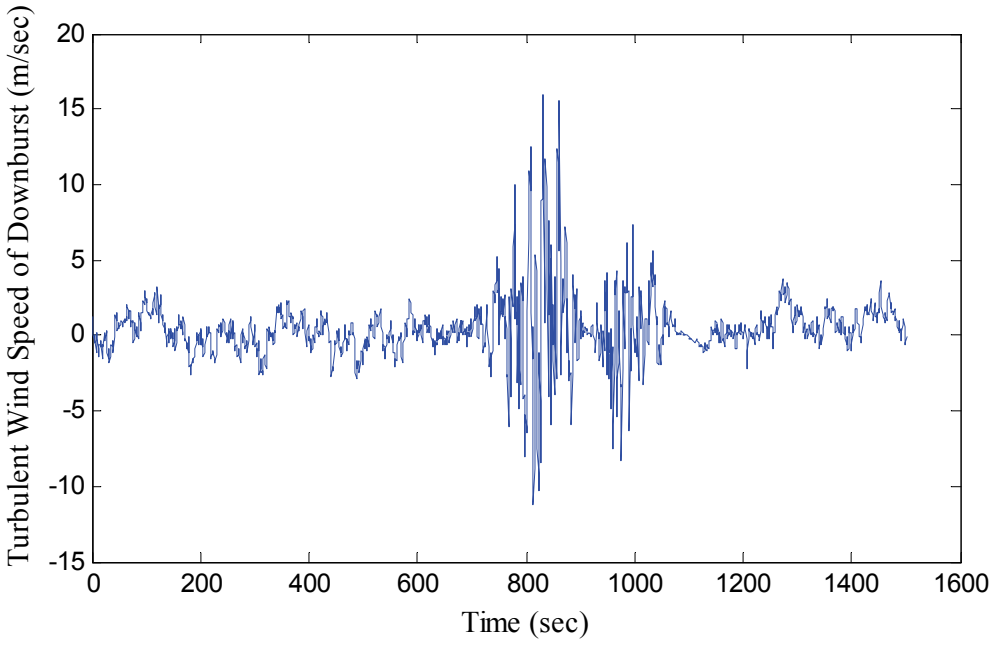

Fig. 10. Turbulent wind speed time history of the generated downburst

Figure 11

Journal of Structural Engineering. Submitted December 15, 2011; accepted August 2, 2012;
posted ahead of print August 13, 2012. doi:10.1061/(ASCE)ST.1943-541X.0000697

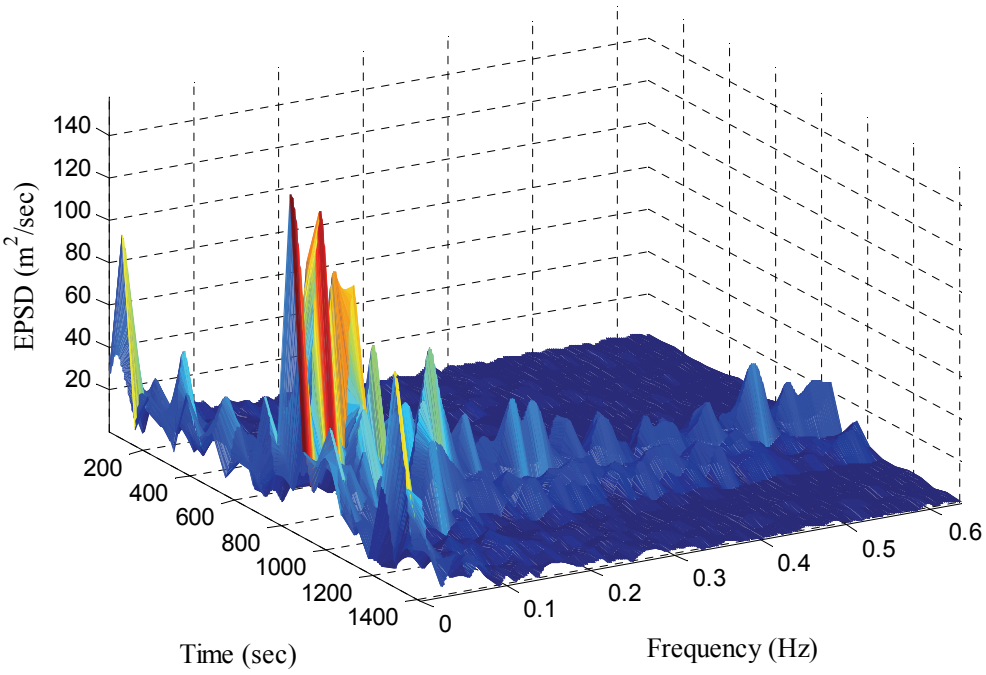

Fig. 11. EPSD function of the generated turbulent wind speed displayed in Fig. 10.

Table 1

Journal of Structural Engineering. Submitted December 15, 2011; accepted August 2, 2012;
posted ahead of print August 13, 2012. doi:10.1061/(ASCE)ST.1943-541X.0000697

Table 1: Derived modulating function corresponding to the wind velocity power spectrum such as Kaimal, Davenport, Harris and Simiu.

Kaimal	***Davenport***	***Harris***	***Simiu***
Power spectrum： $$S(\omega)=\frac{1}{2}\frac{200}{2\pi}u_*^2\frac{z_j}{U_{z_j}}\frac{1}{\left[1+50\frac{\omega\, z_j}{2\pi U_{z_j}}\right]^{5/3}}$$	Power spectrum： $$S(\omega)=4KU_{10}^2\frac{\left(\frac{1200\omega}{2\pi U_{10}}\right)^2}{\omega\left(1+\left(\frac{1200\omega}{2\pi U_{10}}\right)^2\right)^{4/3}}$$	Power spectrum： $$S(\omega)=4u_*^2\frac{\frac{1800\omega}{2\pi U_{10}}}{\omega\left(2+\left(\frac{1800\omega}{2\pi U_{10}}\right)^2\right)^{5/6}}$$	Power spectrum： $$\begin{cases} S(\omega)=\frac{1}{2}\frac{200}{2\pi}u_*^2\frac{z_j}{U_{z_j}}\frac{1}{\left[1+50\frac{\omega\, z_j}{2\pi U_{z_j}}\right]^{5/3}}, & \frac{\omega\, z_j}{2\pi U_{z_j}}\le 0.2 \quad (1) \\ S(\omega)=0.26u_*^2\frac{1}{\omega\left(\frac{\omega\, z_j}{2\pi U_{z_j}}\right)^{2/3}}, & \frac{\omega\, z_j}{2\pi U_{z_j}}>0.2 \quad (2) \end{cases}$$
Modulating function： $$A(\omega,t)=\sqrt{\frac{\tilde{U}_{z_j}(t)}{U_{z_j}}\left[\frac{1+50\frac{\omega\, z_j}{2\pi U_{z_j}}}{1+50\frac{\omega\, z_j}{2\pi\tilde{U}_{z_j}(t)}}\right]^{5/3}}$$	Modulating function： $$A(\omega,t)=\left(\frac{1+\left(\frac{1200\omega}{2\pi U_{10}}\right)^2}{1+\left(\frac{1200\omega}{2\pi\tilde{U}_{10}(t)}\right)^2}\right)^{2/3}$$	Modulating function： $$A(\omega,t)=\sqrt{\frac{\tilde{U}_{10}(t)}{U_{10}}\left(\frac{2+\left(\frac{1800\omega}{2\pi U_{10}}\right)^2}{2+\left(\frac{1800\omega}{2\pi\tilde{U}_{10}(t)}\right)^2}\right)^{5/6}}$$	Modulating function： $$\begin{cases} A(\omega,t)=\sqrt{\frac{\tilde{U}_{z_j}(t)}{U_{z_j}}\left[\frac{1+50\frac{\omega\, z_j}{2\pi U_{z_j}}}{1+50\frac{\omega\, z_j}{2\pi\tilde{U}_{z_j}(t)}}\right]^{5/3}}, & \frac{\omega\, z_j}{2\pi\tilde{U}_{z_j}(t)}\le 0.2 \quad (1) \\ A(t)=\left(\frac{\tilde{U}_{z_j}(t)}{U_z}\right)^{4/3}, & \frac{\omega\, z_j}{2\pi\tilde{U}_{z_j}(t)}>0.2 \quad (2) \end{cases}$$

Table 2

Journal of Structural Engineering. Submitted December 15, 2011; accepted August 2, 2012;
posted ahead of print August 13, 2012. doi:10.1061/(ASCE)ST.1943-541X.0000697

Table 2: Comparisons of the computational efficiency between SSR and SR

Cases	The dividing number of frequency N	The length of simulation time T (s)	Time Consumption TC (s)		$\frac{TC_{SSR}}{TC_{SR}} \times 100$ (%)
			SR	SSR	
1	2048	3216.99	347	58	16.7
2	2048	4823.04	521	89	17.1
3	2048	6430.72	697	118	16.9
4	4096	6430.72	1486	161	10.8
5	8192	6430.72	2833	253	8.9